ELECTROCHEMICAL BEHAVIOUR OF AISI 304 STAINLESS STEEL IN SULFURIC SOLUTION: EFFECTS OF ACID CONCENTRATION

A. Fattah-alhosseini * **and H. Farahani**

* *a.fattah@basu.ac.ir*

Received: May 2013 **Accepted: September 2013**

Assistance Professor, Faculty of Engineering, Bu-Ali Sina University, Hamedan, Iran.

Abstract: *The effects of H_2SO_4 concentration on the electrochemical behaviour of passive films formed on AISI 304 stainless steel were investigated using by potentiodynamic polarization, Mott–Schottky analysis and electrochemical impedance spectroscopy (EIS). Potentiodynamic polarization indicated that the corrosion potentials were found to shift towards negative direction with an increase in solution concentration. Also, the corrosion current densities increase with an increase in solution concentration. Mott–Schottky analysis revealed that the passive films behave as n-type and p-type semiconductors at potentials below and above the flat band potential, respectively. Also, Mott–Schottky analysis indicated that the donor and acceptor densities are in the range 1021 cm^{-3} and increased with solution concentration. EIS data showed that the equivalent circuit $R_s(Q_{dl}[R_{ct}(R_fQ_f)])$ by two time constants is applicable.*

Keywords: *Stainless steel; Concentration; Potentiodynamic polarization; Equivalent circuit; Mott–Schottky.*

1. INTRODUCTION

Stainless steels have many properties such as chemical resistance, mechanical strength, hardness, surface finish, cleanliness and neatness make it a highly valuable material for many industrial applications. These alloys are the most common of the multi-component construction materials used by the chemical and petrochemical industries [1-3]. The higher corrosion resistance of these alloys is due to the presence of passive films (very thin passivating and self-renewable protective layers) formed on the surface. Passive films of metals and alloys are mainly made up of metallic oxides or hydroxides which are envisaged as semiconductors. Consequently, semiconducting properties are often observed on the surfaces of the passivity metals [4-6].

The electrical properties of passive films are expected to be crucially important in understanding the protective characters against corrosion. Mott–Schottky analysis has been widely used to study and characterize the semiconducting properties of the passive films, such as the passive films on steels [7, 8] and stainless steels [9, 10]. Passivity of stainless steel is usually attributed to the formation on the metal surface of a mixture of iron and chromium oxide film with semiconducting behavior. In the last decade, increasing research of the electronic properties of passive films formed on stainless steels has given an important contribution to the understanding of the corrosion behavior of these alloys [11-13].

The film composition, however, varies with both the alloy composition and the pH of the solution used for film formation, and this is expected to affect the semiconducting properties of the passive film [14, 15]. The main effect of an increasing pH on film formation is a thickening of the passive film, basically because iron oxides are more stable in alkaline solutions. Conversely, in acid solutions a chromium-rich oxide film is formed due to slower dissolution of chromium oxide when compared to iron oxide [16, 17].

However, there are limited systematic studies on the effects of solution concentration on the passive behaviour of stainless steel in acidic media. The aim of this paper was to investigate the influence of solution concentration on the passive films formed on AISI 304 stainless steel under open circuit potential conditions using the potentiodynamic polarization and EIS. Also, Mott-Schottky analysis of AISI 304 stainless steel was performed and the defects concentrations were calculated as a function of

solution concentration. The relationship between the defects concentrations and solution concentration are discussed in order to understand the property of the passivation of AISI 304 stainless steel.

2. EXPERIMENTAL PROCEDURES

Specimens were fabricated from AISI 304 stainless steel; the chemical composition is given in the Table 1. All samples were polished mechanically by abrading with wet emery paper up to 1200 grit size on all sides and then were embedded in cold curing epoxy resin. After this, the stainless steels were degreased with acetone, rinsed with distilled water and dried with a stream of air just before immersion. Aerated acidic solutions with three different concentrations were used and the compositions were 0.1 M H_2SO_4, 0.5 M H_2SO_4 and 1.0 M H_2SO_4, respectively. All solutions were made from analytical grade 97% H_2SO_4 and distilled water, and the tests were carried out at ambient temperature.

All electrochemical measurements were performed in a conventional three-electrode cell under aerated conditions. The counter electrode was a Pt plate, and all potentials were measured against Ag/AgCl in saturated KCl. All electrochemical measurements were obtained using μ autolab potentiostat/galvanostat controlled by a personal computer.

Prior to all electrochemical measurements, working electrodes immersed at open circuit potential for 1 h to form a steady-state passive film. Potentiodynamic polarization curves were measured potentiodynamically at a scan rate of 1 mV/s starting from -0.25 V (vs. Ecorr) to 1.2 V. The impedance spectra were measured in a frequency range of 10 mHz –100 KHz at an AC amplitude of 10 mV (rms). The validation of the impedance spectra was performed by checking the linearity condition, i.e. measuring spectra at AC signal amplitudes between 5 and 15 mV (rms). Each electrochemical measurement was repeated at least three times. For EIS data modeling and curve-fitting method, NOVA impedance software was used. Capacitance measurements were carried out on the passive films at a frequency of 1 kHz using a 10 mV ac signal and a step rate of 25 mV, in the cathodic direction.

3. RESULTS AND DISCUSSION

3. 1. Potentiodynamic Polarization

Fig. 1 shows the potentiodynamic polarization curves of AISI 304 stainless steel in 0.1, 0.5 and 1.0 M H_2SO_4. By comparing the polarization curves in different solution, the corrosion potentials were found to shift towards negative direction with an increase in solution concentration. In addition, the corrosion current densities increase with an increase in solution concentration. For all curves, the current increases with potential during the early stage of passivation and the passive currents increases

Table 2. Passivation values of AISI 304 stainless steel immersed in 0.1, 0.5 and 1.0 M H_2SO_4

Solution (M)	E_{corr} (V)	i_{corr} (A cm^{-2})	E_{bp} (V)
0.1	-0.271	2.5×10^{-6}	0.940
0.5	-0.321	8.9×10^{-6}	0.974
1.0	-0.378	3.6×10^{-5}	0.995

Table 1. Chemical compositions of AISI 304 stainless steel.

Elements	Cr	Ni	Mn	Si	C	P	S	Fe
AISI 304 stainless steel/ wt%	19.1	9.35	1.66	0.45	0.08	0.03	0.003	Bal

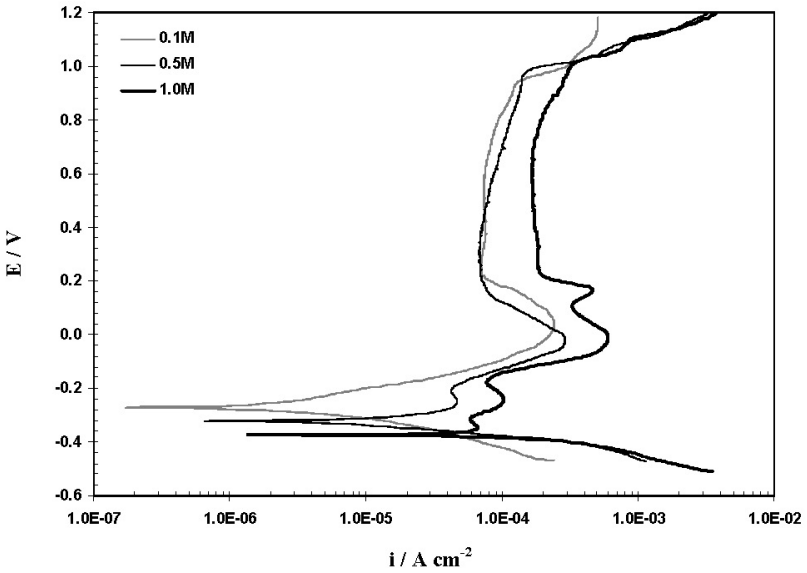

Fig. 1. Potentiodynamic polarization curves at 1 mV/s for AISI 304 stainless steel in solutions with different concentration in H_2SO_4 solution.

with solution concentration. Also, all curves exhibit similar features, with a passive potential range extending from the corrosion potential to the onset of transpassivity. Table 2 summarizes the corrosion potentials (Ecorr), corrosion current densities (icorr) and breakdown potentials (Ebp) of AISI 304 stainless steel in 0.1, 0.5 and 1.0 M H_2SO_4.

3. 2. Mott-Schottky Analysis

The previous study has proved that the outer layer of passive films contains the space charge layer and sustains a potential drop across the film. The charge distribution at the semiconductor/solution is usually determined based on Mott-Schottky relationship by measuring electrode capacitance C, as a function of electrode potential E [18-20]:

$$\frac{1}{C^2} = \frac{2}{\varepsilon\varepsilon_0 e N_D}\left(E - E_{FB} - \frac{kT}{e}\right)$$

for n-type semiconductor (1)

$$\frac{1}{C^2} = -\frac{2}{\varepsilon\varepsilon_0 e N_A}\left(E - E_{FB} - \frac{kT}{e}\right)$$

for p-type semiconductor (2)

where e is the electron charge (-1.602×10^{-19} C),), N_D is the donor density for n–type semiconductor (cm^{-3}), N_A is the accept density for p–type semiconductor (cm^{-3}), ε is the dielectric constant of the passive film, usually taken as 15.6 [21-23]), ε_0 is the vacuum permittivity (8.854×10^{-14} F cm^{-1}), k is the Boltzmann constant (1.38×10^{-23} J K^{-1}), T is the absolute temperature and E_{FB} is the flat band potential. From Eq. (1) N_D can be determined from the slope of the experimental C^{-2} versus E plots, and E_{FB} from the extrapolation of the linear portion to $C^{-2} = 0$. The validity of Mott-Schottky analysis is based on the assumption that the capacitance of the space charge layer is much smaller than the double layer capacitance. Hence, the capacitance determined is mainly from the contribution of the space charge layer. This assumption is reasonable provided that the frequency is high enough.

Fig. 2 shows the Mott-Schottky plots of AISI 304 stainless steel in 0.1, 0.5 and 1.0 M H_2SO_4.

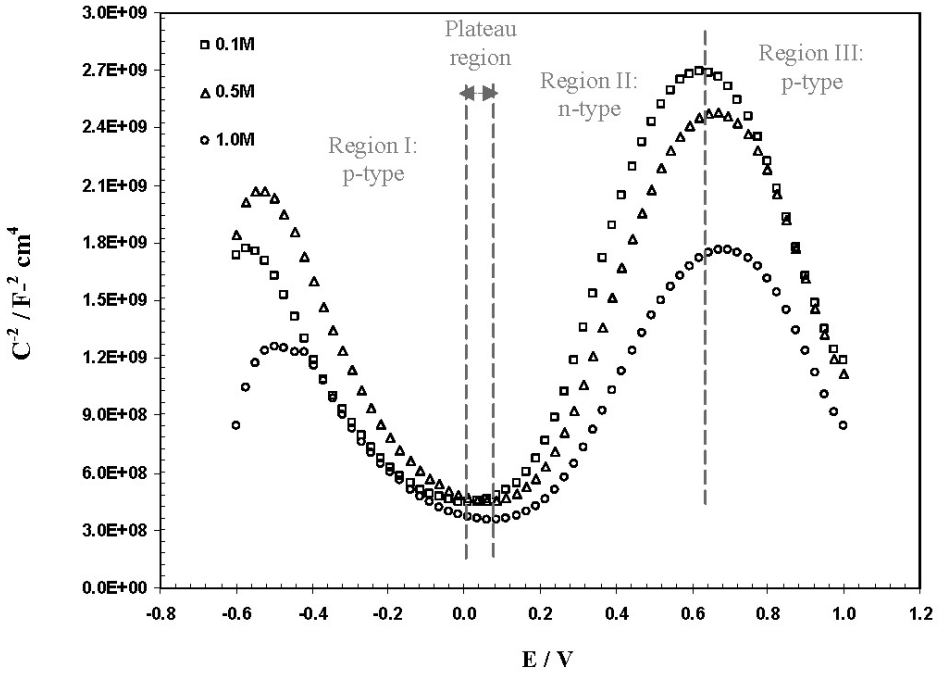

Fig. 2. Mott-Schottky plots of the passive films formed on AISI 304 stainless steel in H_2SO_4 solutions. The electrodes are immersed at open circuit potential for 1 h to form a steady-state passive film.

Firstly, it should be noted that for all concentration, capacitances clearly increase with solution concentration. Secondly, all plots show three regions in which a linear relationship between C^{-2} and E can be observed. The negative slopes in region I are attributed to a p-type behaviour, probably due to the presence of Cr_2O_3, FeO and NiO on the passive films [24]. Region II presents positive slopes, which depicts an n-type semiconducting behaviour. Finally, the negative slopes in region III are attributed to p-type behaviour, with a peak at around 0.65 V. This feature is usually explained in terms of a strong dependence of the Faradaic current on potential in the transpaasive region [24]. In this sense, the behaviour of capacitance at high potentials near the transpaasive region is attributed to the development of an inversion layer as a result of an increasing concentration in the valence band (high valency Cr in the film prior to transpaasive dissolution).

In all plots, straight lines with a negative and positive slope separated by a narrow potential plateau region (0.0 to 0.1 V), where the flat band potential (E_{fb}) is observed. In the potential more than 0.1 V, the positive slope indicates n-type behavior and in the potential less than 0.0 V, the negative slope is representative of the behavior of a p-type behavior. Thus, Mott-Schottky analysis show that the passive films formed on this stainless steel behave as n-type and p-type semiconductors above and below the flat band potential, respectively. This behavior implies that the passive films have a duplex structure, which would not have been realized if the measurements were restricted to only the more anodic potentials. Early studies of the bipolar duplex structures of passive films on stainless steels are attributed to Sato [25], and since then, other investigations have given credence to this observation [26, 27]. It is widely accepted that the inner part of the passive film, which has a p-type behavior, consists mainly of Cr oxides, whereas the outer region, with the features of an n-type behavior, is predominantly Fe oxides. Contributions to the p-type behavior at $E < E_{fb}$ are restricted to the inner Cr oxide layer, with negligible contributions from the Fe oxides in the

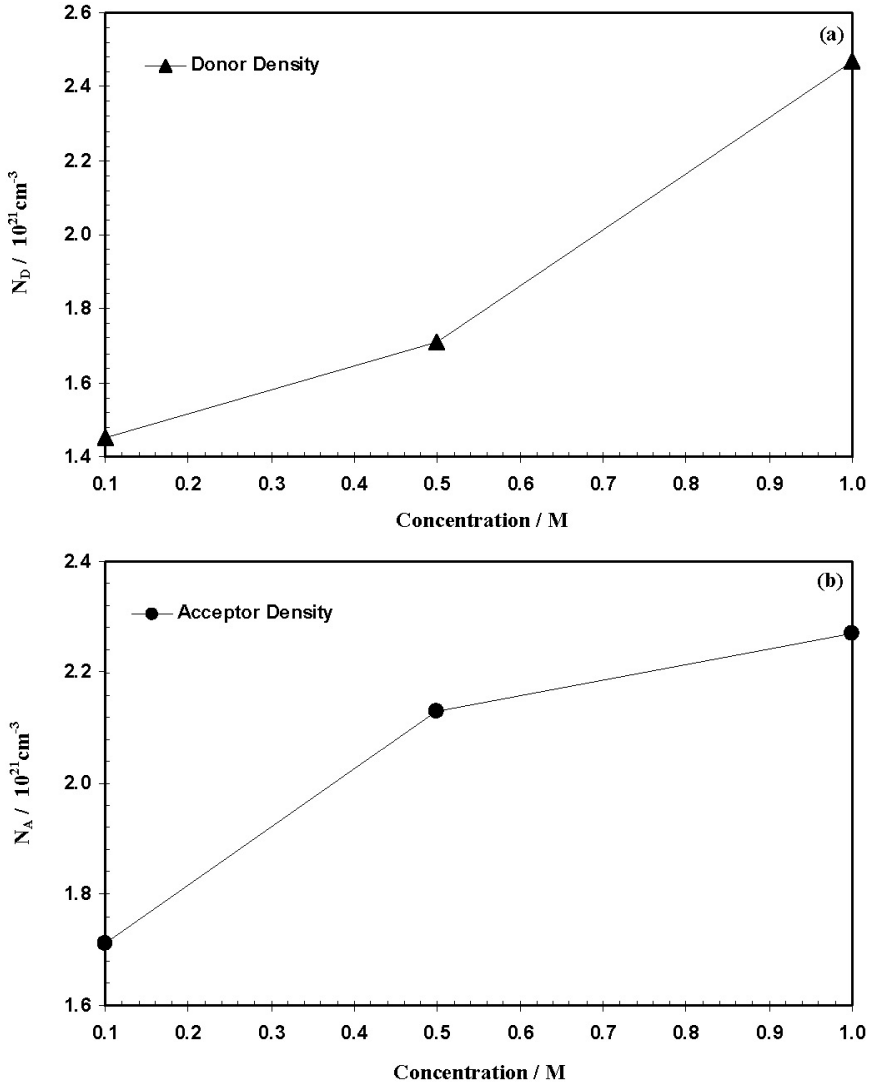

Fig. 3. (a) Donor and (b) acceptor densities of the passive films formed on AISI 304 stainless steel in sulfuric acid solutions as a function of concentration.

outer part of the film, whereas the n-type behavior at $E > E_{fb}$ depends exclusively on the outer Fe oxide region with no contribution from the Cr oxide region [27].

According to Eq. (1), donor density has been determined from the positive slopes in region II of Fig. 2. Also, acceptor density has been calculated from the negative slopes in region III of Fig. 2, according to Eq. (2). Fig. 3(a) and (b) shows the calculated donor and acceptor densities for the films formed on AISI 304 stainless steel in 0.1, 0.5 and 1.0 M H_2SO_4. The orders of magnitude are around 1021 cm^{-3} and are comparable to those reported in other studies [27]. According to Fig. 3(a) and (b), the donor and acceptor densities increase with solution concentration, respectively. Changes in donor and acceptor densities correspond to the non-stoichiometry defects in the passive film. Therefore, it can be concluded that the passive film on AISI 304 stainless steel is disordered and becomes more visible at higher concentration. Based on Point defect model (PDM) the donors or acceptors in semiconducting passive layers are

point defects, as explained briefly in the part 3.3.

3. 3. PDM

Although many models and theories have been proposed to explain the passivation of materials, a satisfactory description of the phenomenon is still in lack. The PDM [28, 29], which was developed by Macdonald et al., described the growth and breakdown of passive film qualitatively from a microscopic perspective. This model is based on the assumption that the passive film contains a high concentration of point defects, such as oxygen vacancies and metal cation vacancies. The growth and breakdown of the passive film involves the migration of these point defects under the influence of the electrostatic field in the film. Thus, the key parameters in determining the transport of point defects and hence the kinetics of film growth is the density of the defects in film [28, 29].

The PDM [28, 29] postulates that passive films are bilayer structures comprising a highly defective barrier layer that grows into the metal and an outer layer that forms via the hydrolysis of cations transmitted through the barrier layer and the subsequent precipitation of a hydroxide, oxyhydroxide, or oxide, depending upon the formation conditions. The outer layer may also form by transformation of the outer surface of the barrier layer itself, provided that the outer layer is thermodynamically more stable than the barrier layer.

The PDM further postulates that the point defects present in a barrier layer are, in general, cation vacancies ($V_M^{\chi'}$), oxygen vacancies ($V_O^{\cdot\cdot}$), and cation interstitials ($M_i^{\chi+}$), as designated by the Kroger-Vink notation. The defect structure of the barrier layer can be understood in terms of the set of defect generation and annihilation reactions occurring at the metal/barrier layer interface and at the barrier layer- solution interface, as depicted in Fig. 4 [28, 29].

Cation vacancies are electron acceptors, thereby doping the barrier layer p-type, whereas oxygen vacancies and metal interstitials are electron donors, resulting in n-type doping. Thus,

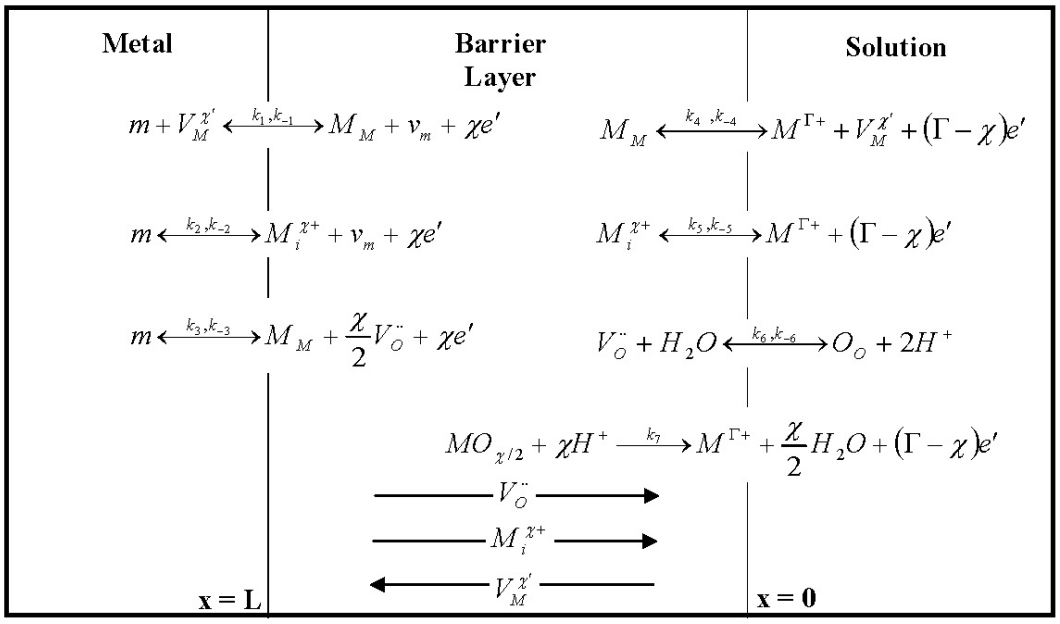

Fig. 4. Interfacial defect generation-annihilation reactions that are postulated to occur in the growth of passive films according to the PDM. m = metal atom, M_M = metal cation on the metal sublattice, O_O = oxygen anion on the oxygen sublattice, $M^{\Gamma+}$= metal cation in solution [28, 29].

on pure metals, the barrier layer is essentially a highly doped, defect semiconductor, as demonstrated by Mott-Schottky analysis, for example. Not unexpectedly, the situation with regard to alloys is somewhat more complicated than that for the pure metals, because substitution of other metal cations, having oxidation states different from the host, on the cation sublattice may also impact the electronic defect structure of the film. Thus, while the barrier layers on pure chromium and on Fe-Cr-Ni alloys are commonly described as being "defective Cr_2O_3," that on pure chromium is normally p-type in electronic character, while those on the stainless steels are n-type. It is not known whether this difference is due to doping of the barrier layer by other alloying elements (Ni, Fe), as indicated above, or is due to the inhibition of cation vacancy generation relative to the generation of oxygen vacancies and metal interstitials, in the barrier layer on the alloys compared with that on pure chromium [28, 29]. According to the PDM, the flux of oxygen vacancy and/or cation interstitials (Cr^{2+}, Cr^{3+}, Fe^{2+}, and Ni^{2+}) through the passive film is essential to the film growth process. In this concept, the dominant point defects in the passive film at low potential passive region are considered to be oxygen vacancies and/or cation interstitials.

3. 4. EIS Measurements

Fig. 5 presents the EIS spectra (Nyquist plots) obtained for the AISI 304 stainless steel at the open circuit potential after 1 h immersion in H_2SO_4 solutions. In Fig. 5, all Nyquist plots have the same shape and it is clear that the overall interfacial impedance is large (~ kΩ cm^2) and decreases with solution concentration. Nyquist plot displays two capacitive loops. The high-frequency capacitive loop is associated to the charge transfer resistance and the second loop in the low-frequency domain reflects the relaxation of adsorbed intermediates. These intermediates include [FeOH]ads and [FeH]ads. It was pointed out that in strong acidic solution and in the potential

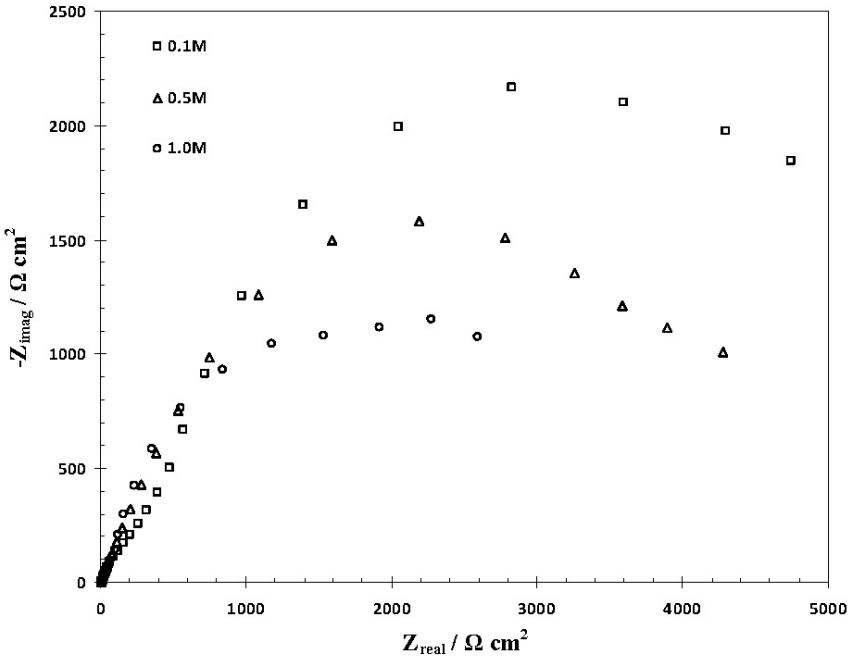

Fig. 5. Nyquist plots of AISI 304 stainless steel in 0.1, 0.5 and 1.0 M H_2SO_4. The electrodes are immersed at open circuit potential for 1 h.

region near the open-circuit corrosion potential, both the anodic iron dissolution and the hydrogen evolution occur simultaneously on the electrode surface. The appearance of the second loop in the low-frequency indicates that the kinetics of the dissolution of the surface oxide film is limited by diffusion of the oxidation products [30].

3. 5. Fitting the Impedance Data

Literature proposes different models of equivalent circuits to interpret the impedance data on passive films formed on stainless steels in acidic media. The simplest equivalent circuit used for analysis and fitting the impedance data is shown in Fig. 6. This equivalent circuit composed by one time constant as proposed by Pardo et al. [31] to describe the behaviour of AISI 304 and 316 stainless steels in H_2SO_4 solutions. In this circuit, as shown in Fig. 6, R_s is in a series with a parallel combination of Q_{dl} (double layer constant phase element) and R_{ct} (charge transfer resistance). Q_{dl} is used instead of pure capacitance to account for the depression of the capacitive loop which is usually attributed to surface heterogeneity. The impedance of the

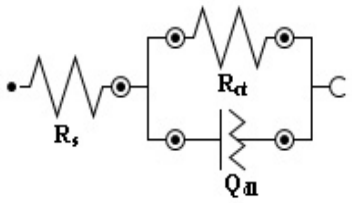

Fig. 6. The simplest equivalent circuit tested to model the experimental EIS data.

constant phase element (Q) is presented by

$$Z_Q = \left[Y_0 (j\omega)^n\right]^{-1} \quad (3)$$

Where n is associated with the roughness of the electrode surface and Y_0 is a frequency-independent real constant representing the total capacitance of the Q. When n = 1, it means that Q is equivalent to a pure capacitor and $Y_0 = C$ [32]. As shown in Fig. 7, this model could not fit the impedance data obtained in the present work.

The best equivalent circuit used for analysis and fitting the impedance data is shown in Fig. 8.

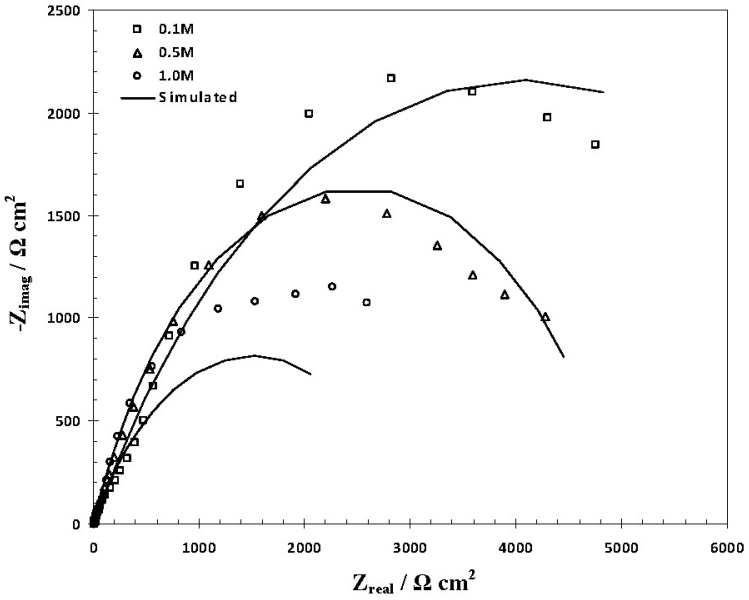

Fig. 7. The fitting results of Nyquist plots of AISI 304 stainless steel in 0.1, 0.5 and 1.0 M H_2SO_4.

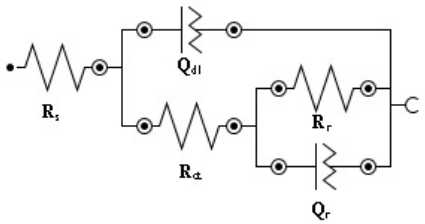

Fig. 8. The best equivalent circuit tested to model the experimental EIS data with two hierarchically distributed time constants.

This equivalent circuit has been reported as excellent to model the passivation of stainless steels in acidic media [24, 33]. This circuit presents two time constants. The interpretation suggested for the circuit elements is the following one: the high frequencies (R_{ct}: charge transfer resistance, Q_{dl}: double layer constant phase element) time constant can be associated with the charge transfer process and the low frequencies (R_r, Q_r) time constant can be correlated with the redox processes taking place in the surface film. This equivalent circuit was provided best fitting for the impedance data obtained in the present work as shown in Fig. 9. Table 3 presents the best fitting parameters obtained for the films formed on AISI 304 stainless steel immersed in 0.1, 0.5 and 1.0 M H_2SO_4 solutions. Concerning the evolution with solution concentration, the fitting parameters R_{ct} and Y_{0dl} for the films formed on AISI 304 stainless steel are affected. R_{ct} suffers decrease, and the admittance of Q_{dl} seems very close to the values expected for a double layer capacitance. Also, the fitting parameters R_r and Y_{0r} are affected by solution concentration. R_r decreases with a tendency to increase with solution concentration.

Polarization resistance, R_p ($R_p = R_{ct} + R_r$), where R_{ct} and R_r were parameters from the fitting procedure, is commonly used as a measure of the resistance of a metal to the corrosion damage [34]. The calculated R_p for the passive films formed on AISI 304 stainless steel immersed in 0.1, 0.5 and 1.0 M H_2SO_4 solutions is shown in Fig. 10. As shown, the polarization resistance decreases with solution concentration. Generally, the corrosion mechanism of the acid dissolution of stainless steel is dependent not only on the hydrogen ion concentration but also on the counter ion of the acid. It is suggested that the extent of adsorption of SO_4^{2-} ion on the electrode

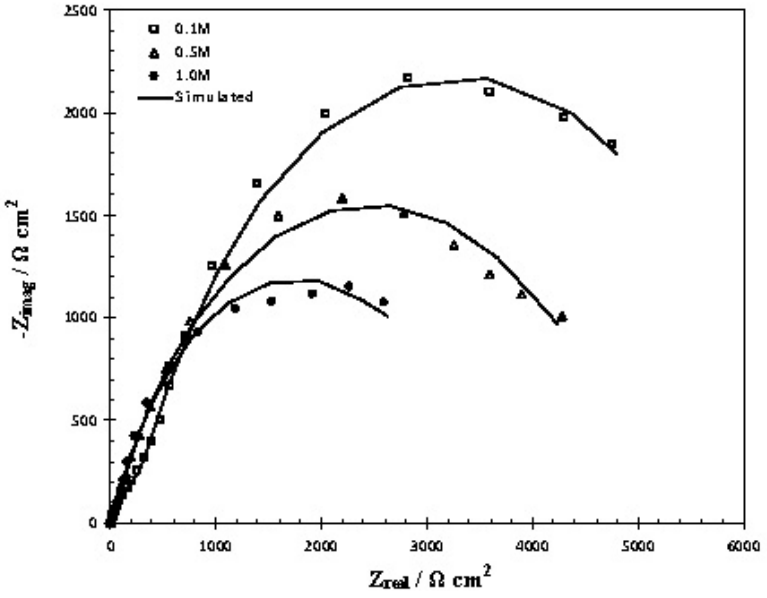

Fig. 9. The fitting results of Nyquist plots of AISI 304 stainless steel in 0.1, 0.5 and 1.0 M H_2SO_4.

Table 3. Best fitting parameters for the impedance spectra of AISI 304 stainless steel in 0.1, 0.5 and 1.0 M H_2SO_4.

Solution (M)	R_s (Ω cm^2)	R_{ct} (Ω cm^2)	Y_{0dl} (μF cm^{-2} s^{n-1})	n_{dl}	R_r (Ω cm^2)	Y_{0r} (μF cm^{-2} s^{n-1})	n_r
0.1	11.79	462.52	160.88	0.793	5884.6	486.56	0.787
0.5	7.55	80.69	59.23	0.955	4935.2	314.66	0.675
1.0	5.28	47.01	171.54	0.826	3463.1	855.17	0.752

greatly determines the corrosion rate. It was reported [35] that SO_4^{2-} has a low tendency to adsorb on the steel surface. Hence the concentration of surface complex formed is not sufficient to cover the electrode surface from the solution or the complex is not so stable that it is desorbed from the surface.

4. CONCLUSIONS

The semiconductor properties of passive films formed on AISI 304 stainless steel in H_2SO_4 solutions under open circuit potential conditions were investigated in the present work. Conclusions drawn from the study are as follows:

1. The polarization curves suggested that AISI 304 stainless steel showed comparable passive behaviour in sulfuric solutions.
2. By comparing the polarization curves in different solution, the corrosion potentials were found to shift towards negative direction with an increase in solution concentration. Also, the corrosion current densities increase with an increase in solution concentration
3. Mott–Schottky analysis revealed that the existence of a duplex passive film structure composed of two oxide layers of distinct semiconductivities (n-type and p-type).
4. Based on the Mott–Schottky analysis, it was shown that donor and acceptor densities are in the range of 1021 cm^{-3} and increase with solution concentration.
5. EIS results showed that the best electrical equivalent circuit presents two time constants: The high frequencies (R_{ct}: charge transfer resistance, Q_{dl}: double layer constant phase element) time constant can be associated with the charge transfer process and the low frequencies (R_r, Q_r) time constant can be correlated with the redox processes taking place in the surface film.
6. Based on the EIS analysis, it was shown that the polarization resistance decreases with solution concentration.

REFERENCES

1. Yamamoto, T., Fushimi, K., Seo, M., Tsuri, S., Adachi, T., and Habazaki, H., "Depassivation–repassivation behavior of type-312L stainless steel in NaCl solution investigated by the micro-indentation", Corros. Sci., 2009, 51, 1545.
2. Pardo, A., Merino, M. C., Coy, A. E., Viejo, F., Carboneras, M., and Arrabal, R., "Influence of Ti, C and N concentration on the intergranular corrosion behaviour of AISI 316Ti and 321 stainless steels", Acta Materialia, 2007, 55, 2239.
3. Chen, Y. Y., Liou, Y. M., and Shih, H. C., "Stress corrosion cracking of type 321 stainless steels in simulated petrochemical process environments containing hydrogen sulfide and chloride", Mater. Sci. Eng. A, 2005, 407,114.
4. Hakiki, N. E., Da Cunha Belo, M., Simões, A. M. P., and Ferreira, M. G. S., "Semiconducting

properties of passive films on stainless steel. Influence of the alloying elements", J Electrochem. Soc., 1998, 145, 3821.
5. Da Cunha Belo, M., Hakiki, N. E., and Ferreira, M. G. S., "Semiconducting properties of passive films formed on nickel-base alloys type alloy 600". Influence of the alloying elements, Electrochim. Acta, 1999, 44, 2473.
6. Sugimoto, K., and Sawada, Y., "The role of molibdenum additions to austenitc stainless steels in the inhibition of pitting in acid chloride solutions", Corros. Sci., 1997, 17, 425.
7. Fujimoto, S., and Tsuchiya, H., "Semiconductor properties and protective role of passive films of iron base alloys", Corros. Sci., 2007, 49, 195.
8. Wielant, J., Goossens, V., Hausbrand, R., and Terryn, H., "Electronic properties of thermally formed thin iron oxide films", Electrochim. Acta, 2007, 52, 7617.
9. Amri, J., Souier, T., Malki, B., and Baroux, B., "Effect of the final annealing of cold rolled stainless steels sheets on the electronic properties and pit nucleation resistance of passive films", Corros. Sci., 2008, 50, 431.
10. Ningshen, S., Mudali, U. K., Mittal, V. K., and Khatak, H. S., "Semiconducting and passive film properties of nitrogen-containing type 316LN stainless steels", Corros. Sci., 2007, 49, 481.
11. Simões, A. M. P., Ferreira, M. G. S., Rondot, B., and Da Cunha Belo, M., "Study of Passive Films Formed on AISI 304 Stainless Steel by Impedance Measurements and Photoelectrochemistry", J. Electrochem. Soc., 1990, 137, 82.
12. Mischler, S., Vogel, A., Mathieu, H., and Landolt, D., "The chemical composition of the passive film on Fe-24Cr and Fe-24Cr-11Mo studied by AES", XPS and SIMS, Corros Sci., 1991, 32, 925.
13. Montemor, M. F., Ferreira, M. G. S., Hakiki, N. E., and Da Cunha Belo, M., "Chemical composition and electronic structure of the oxide films formed on 316L stainless steel and nickel based alloys in high temperature aqueous environments", Corros. Sci., 2000, 42, 1635.
14. Sunseri, C., Piazza, S., and Di Quarto, F., "Photocurrent Spectroscopic Investigations of Passive Films on Chromium", J. Electrochem. Soc., 1990, 137, 2411.
15. Carmezim, M. J., Simões, A. M., Figueiredo, M. O., and Da Cunha Belo, M., "Electrochemical behaviour of thermally treated Cr- oxide films deposited on stainless steels", Corros. Sci., 2002, 44, 451.
16. Haupt, S., and Strehblow, H. H., "A combined surface analytical and electrochemical study of the formation of passive layers on FeCr alloys in 0.5 M H_2SO_4", Corros. Sci., 1995, 37, 43.
17. Cardoso, M. V., Amaral, S. T., and Martini, E. M. A., "Temperature effect in the corrosion resistance of Ni–Fe–Cr alloy in chloride medium", Corros. Sci., 2008, 50, 2429.
18. Dutta, R. S., Dey, G. K., and De, P. K., "Characterization of microstructure and corrosion properties of cold worked Alloy 800", Corros. Sci., 2006, 48, 2711.
19. Gaben, F., Vuillemin, B., and Oltra, R., "Influence of the Chemical Composition and Electronic Structure of Passive Films Grown on 316L SS on Their Transient Electrochemical Behavior", J. Electrochem. Soc., 2004, 151, B595.
20. Macak, J., Sajdl, P., Kucera, P., Novotny, R., and Vosta, J., "In situ electrochemical impedance and noise measurements of corroding stainless steel in high temperature water", Electrochim. Acta, 2006, 51, 3566.
21. Qiao, Y. X., Zheng, Y. G., Ke, W., and Okafor, P. C., "Electrochemical behaviour of high nitrogen stainless steel in acidic solutions", Corros. Sci., 2009, 51, 979.
22. Yang, Y., Guo L. j., and Liu, H., "Effect of fluoride ions on corrosion behavior of SS304L in simulated proton exchange membrane fuel cell (PEMFC) cathode environments", J. Power Sour., 2010, 195, 5651.
23. Li, N., Li, Y., Wang, S., and Wang, F., "Electrochemical corrosion behavior of nanocrystallized bulk 304 stainless steel", Electrochim. Acta, 2006, 52, 760.
24. Escrivà-Cerdán, C., Blasco-Tamarit, E., García-García, D. M., García-Antóna, J., and Guenbour, A., "Effect of potential formation on the electrochemical behaviour of a highly alloyed austenitic stainless steel in contaminated phosphoric acid at different temperatures", Electrochim. Acta, 2012, 80,

248.
25. Sato, N., "An overview of passivity of metals", Corros. Sci., 1990, 31, 1.
26. Ferreira, M. G. S., Hakiki, N. E., Goodlet, G., Faty, S., and Simoes, A. M. P., Da Cunha Belo, M., "Influence of the temperature of film formation on the electronic structure of oxide films formed on 304 stainless steel", Electrochim. Acta, 2001, 46, 3767.
27. Oguzie, E. E., Li, J., Liu, Y., Chen, D., Li, Y., Yang, K., and Wang, F., "The effect of Cu addition on the electrochemical corrosion and passivation behavior of stainless steels", Electrochim. Acta, 2010, 55, 5028.
28. Macdonald D. D., "On the existence of our metals-based civilization I. Phase-space analysis", J. Electrochem. Soc., 2006, 153, B213.
29. Macdonald, D. D., "On the tenuous nature of passivity and its role in the isolation of HLNW", J. Nucl. Mater., 2008, 379, 24.
30. Ma, H., Cheng, X., Chen, S., Wang, C., Zhang, J., and Yang, H., "An ac impedance study of the anodic dissolution of iron in sulfuric acid solutions containing hydrogen sulfide", J. Electroanal. Chem., 1998, 451, 11.
31. Pardo, A., Merino, M. C., Carboneras, M., Viejo, F., Arrabal, R., and Munoz, J., "Influence of Cu and Sn content in the corrosion of AISI 304 and 316 stainless steels in H_2SO_4", Corros. Sci., 2006, 48, 1075.
32. Ma, H., Cheng, X., Li, G., Chen, S., Quan, Z., Zhao, S., and Niu, L., "The influence of hydrogen sulfide on corrosion of iron under different conditions", Corros. Sci., 2000, 42, 1669.
33. Metikoš-Hukovic, M., Babic, R., Grubac, Z., Petrovic, Z., and Lajçi, N., "High corrosion resistance of austenitic stainless steel alloyed with nitrogen in an acid solution", Corros. Sci., 2011, 53, 2176.
34. Luo, H., Dong, C. F., Li, X. G., and Xiao, K., "The electrochemical behaviour of 2205 duplex stainless steel in alkaline solutions with different pH in the presence of chloride", Electrochim. Acta, 2012, 64, 211.
35. Abd El-Maksoud, S. S., "The effect of hexadecyl pyridinium bromide and hexadecyl trimethyl ammonium bromide on the behaviour of iron and copper in acidic solutions", J. Electroanal. Chem., 2004, 565, 321.